

Effect of acrylic acid feed contents of microgels on catalytic activity of silver nanoparticles fabricated hybrid microgels

Zahoor H. FAROOQI^{1,*}, Shanza Rauf KHAN¹, Robina BEGUM², Farah KANWAL¹, Ahsan SHARIF¹, Ejaz AHMED¹, Shumaila MAJEED¹, Kiran IJAZ¹, Aysha IJAZ¹

¹Institute of Chemistry, University of the Punjab, New Campus, Lahore, Pakistan

²Centre for Undergraduate Studies, University of the Punjab, New Campus Lahore, Pakistan

Received: 17.06.2014 • Accepted: 19.08.2014 • Published Online: 23.01.2015 • Printed: 20.02.2015

Abstract: We synthesized poly(N-isopropylacrylamide-co-acrylic acid) microgels with 1, 3, 5, and 7 mol percentage of acrylic acid. Silver nanoparticles were fabricated inside these microgels at room temperature. Pure microgels were characterized by Fourier transform infrared (FTIR) spectroscopy and dynamic light scattering (DLS). Hybrid microgels were characterized by UV-Visible spectroscopy. The size of the silver nanoparticles increased with an increase in the content of acrylic acid. Catalytic activity of these hybrid microgels was investigated using UV-Visible spectrophotometry. Induction time decreased from 8.8 to 2.6 min and the value of apparent rate constant decreased from 0.226 to 0.109 min⁻¹, when the content of acrylic acid was increased from 1 to 7 mol %. This decrease in induction time was due to decrease in the surface area of nanoparticles present within the microgels with an increase in the feed contents of acrylic acid. The decrease in the value of apparent rate constant was due to an increase in the size of nanoparticles fabricated within the microgels with an increase in mol percentage of acrylic acid. The linear relation between apparent rate constant and feed contents of acrylic acid can be used for quantitative analysis of contents of acrylic acid present in polymer microgels.

Key words: Microgels, nanoparticles, hybrid microgel, catalytic activity

1. Introduction

Metal nanoparticles have gained a lot of attention as catalysts due to their size and shape dependent properties.¹⁻⁷ Silver (Ag),^{8,9} platinum (Pt),¹⁰ copper (Cu),^{11,12} nickel (Ni),^{13,14} iron (Fe),¹⁵ and gold (Au)^{16,17} metal nanoparticles have been extensively used as catalysts in various reactions. For example, p-nitrophenol (p-NP),^{9,18} nitrobenzene (NB),^{19,20} o-nitrophenol (o-NP)^{21,22} and m-nitrophenol²² can be reduced in aqueous medium using metal nanoparticles as catalysts. Aggregation or coagulation of nanoparticles limits their activity in the field of catalysis, because catalysis is a surface phenomenon and coagulation of nanoparticles results in a decrease in surface area.⁸ A capping agent or a stabilizer in the form of polymer or surfactant is mostly used to avoid aggregation of nanoparticles.²³ Polymer networks in the shape of polyelectrolyte brushes,¹⁸ microgels,⁹ core-shell networks,^{24,25} and dendrimers^{26,27} are good carriers for nanoparticles as well as good microreactors for synthesis of nanoparticles. Among these systems, microgels are more useful for these purposes. Microgels can be used as microreactors to synthesize metal and metal oxide nanoparticles.²⁸ The size and shape of nanoparticles can be controlled by controlling the crosslinking density and void size of polymer microgels. Metal nanoparticles

*Correspondence: zhfarooqi@gmail.com

fabricated microgel has the properties of both nanoparticles and microgels. The catalytic and optical properties of metal nanoparticles can be tuned by change in environment of smart hybrid microgels.^{29–31} The reactants can easily diffuse through an open polymer network towards the nanoparticle catalysts. The swelling/deswelling of microgel particles in the presence of different stimuli can control the diffusion of reactants toward the surface of metal nanoparticles. The hybrid polymer microgels can be recycled by simple centrifugation method.

Due to these qualities, hybrid microgels are largely used as catalysts.^{9,12} People working in this area are not only interested in the study of catalysis by hybrid microgels, but they also want to modulate the rate of catalysis by changing external parameters. By changing these parameters, rate of catalysis can be modulated.³² Liu et al. studied the effect of temperature on catalytic reduction of p-NP by employing silver-poly(N-isopropylacrylamide) [Ag-p(NIPAM)] hybrid microgels as catalyst.²⁹ Xie et al. prepared hollow p(NIPAM) microspheres for fabrication of Ag nanoparticles of different sizes and employed these hybrid systems as catalyst for reduction of p-NP.³⁰ They found that an increase in the concentration of metal salt precursor increases the size of metal nanoparticles and decreases the catalytic activity. Moreover, the effects of different concentrations of catalyst and sodium borohydride (NaBH_4) on catalytic reduction of p-NP and o-NP were studied by Sahiner et al. using cobalt-poly(2-acrylamido-2-methyl-1-propanesulfonic acid) hybrid microgels as catalyst.³¹ Thus all the above parameters have been studied extensively,^{29–31,33} but mol percentage of ionic monomer can be a new parameter that can be used to modulate the rate of catalysis. To the best of our knowledge, no one has yet reported this parameter in the field of catalysis by hybrid microgels. Thus we are reporting mol percentage of AAc as a new parameter for modulation of catalysis of p-NP by silver-poly(N-isopropylacrylamide-co-acrylic acid) [Ag-p(NIPAM-co-AAc)] hybrid microgels. It has been reported that mol percentage of AAc can affect the swelling ratio of microgels. Kratz et al. prepared p(NIPAM-co-AAc) microgels with 1, 3, 5, and 10 mol percentage of AAc.³⁴ They reported that charge density within the polymer network increases by increasing mol percentage of AAc. They also reported that the hydrodynamic radius of microgels having 10 mol percentage of AAc is greater compared to microgels having 3 mol percentage of AAc at pH 10. We thought that if feed contents of AAc affect the swelling ratio of microgels then they should affect the size and catalytic activity of Ag nanoparticles fabricated inside the microgels. Here we report the synthesis of compact Ag nanoparticles. The surface area of these nanoparticles can be increased by making them hollow. People are working on the synthesis of such complex structures and so these structures can prove to be useful for catalysis in future.^{35–37}

In this research, we studied the effect of mol percentage of AAc on rate of catalytic reduction of p-NP into p-aminophenol (p-AP). For this purpose, initially we synthesized 4 different samples of p(NIPAM-co-AAc) microgels having different content of AAc. Then we fabricated Ag nanoparticles inside these microgels using in vivo reduction. Then we employed these hybrid microgels as catalysts for reduction of p-NP in aqueous medium to investigate the effect of feed contents of AAc on the value of apparent rate constant (k_{app}).

2. Results and discussion

2.1. Fourier transform infrared spectroscopy (FTIR) of p(NIPAM-co-AAc) microgels

The FTIR spectrum of the 7-AAc microgel sample is shown in Figure 1 in which characteristic bands of different functional groups of monomers and crosslinker are present. Thus this FTIR spectrum confirms that polymerization occurred and monomers were incorporated within the polymer network. A characteristic band of N–H stretching is shown around 2972.31 cm^{-1} ; this confirms the presence of NIPAM and BIS in polymer. Distinctive bands of O–H and C–O of AAc are shown at around 3419.79 and 1382.96 cm^{-1} . Bands at around

1560.41 and 1456.26 cm^{-1} represent NH_2 and CH_2 bending vibrations.³⁸ A wide characteristic band of the carbonyl ($\text{C}=\text{O}$) functional group is shown at 1624 cm^{-1} .³⁹ No characteristic band of the $\text{C}=\text{C}$ bond is present at 1600 cm^{-1} , which shows that polymerization has occurred at the reactive site of the carbon-carbon double bond; thus unreacted monomers are not present in the sample.⁹ Van Gough et al. have also reported a similar FTIR spectrum of p(NIPAM-co-AAc) microgels.⁴⁰ Moreover, Yu et al. have obtained a similar FTIR spectrum for p(NIPAM-co-AAc) sensitive membranes.⁴¹

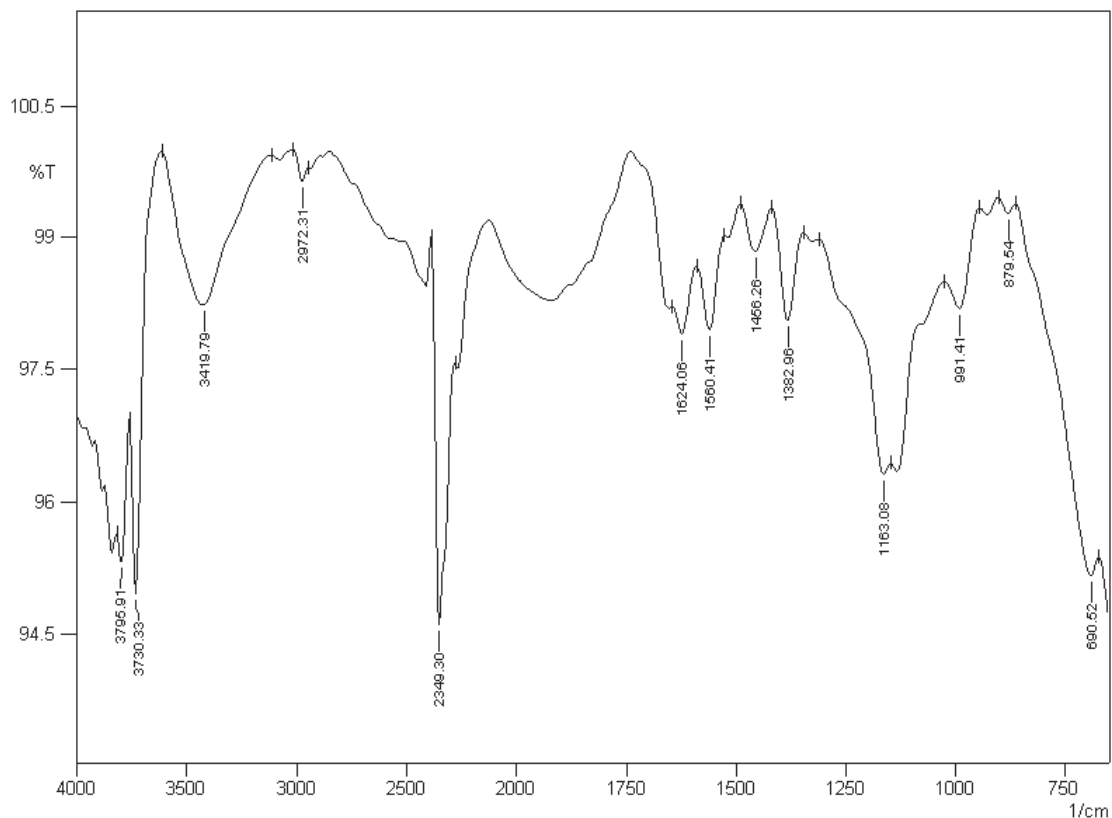


Figure 1. FTIR spectrum of 7-AAc sample of p(NIPAM-co-AAc) microgels.

2.2. DLS study of p(NIPAM-co-AAc) microgels

The plot of pH sensitivity of the 7-AAc sample of p(NIPAM-co-AAc) microgels at 22 °C is shown in Figure 2. Figure 2 shows that the hydrodynamic radius (R_h) of microgels increases with an increase in pH at 22 °C. The increase in the value of R_h with an increase in pH confirms that the particle size of microgels increases with pH. The shape of the curve confirms that this increase in particle size is uniform. The $\text{p}K_a$ of AAc is approximately 4.5.⁴² When pH is less than the $\text{p}K_a$ of AAc, the value of R_h is small because carboxyl groups ($-\text{COOH}$) are in protonated state and electrostatic repulsions are absent. When the pH of the medium is around the $\text{p}K_a$ of AAc, $-\text{COOH}$ ionizes and converts into carboxylate ions ($-\text{COO}^-$). Thus electrostatic repulsions among carboxylate groups develop and push the polymer network apart, water rushes inward, and particle size increases. In addition, the more hydrophilic nature of ionized carboxylate ions as compared to protonated carboxyl groups also attracts water molecules with greater force inward and causes an increase in

particle size.⁴³ When the pH of the solution is above 7, all carboxyl groups have ionized; thus no further increase in R_h value is observed with a further increase in pH. All samples of microgels, which have different AAc feed content, were prepared by the same method using the same monomers; thus all samples possess a similar trend of pH sensitivity. That is why it is confirmed that the polymer network did not offer any resistance against diffusion of reagents (p-NP and NaBH_4) towards the surface of nanoparticles when microgels were employed for catalytic applications at high pH and low temperature. Therefore, the catalysis of p-NP is studied at 21 °C in basic medium (as discussed below in section 2.5. of this manuscript).

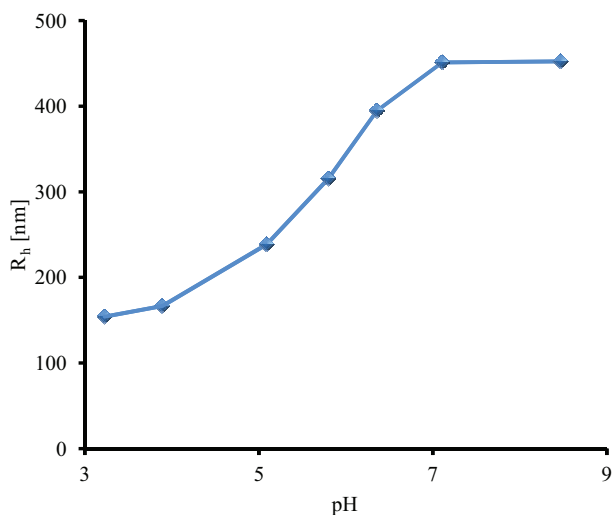


Figure 2. Plot of pH sensitivity of 7-AAc sample of p(NIPAM-co-AAc) microgels at 22 °C.

2.3. Growth of silver nanoparticles within p(NIPAM-co-AAc) microgels

In this study, Ag nanoparticles were in situ synthesized by chemical reduction method using p(NIPAM-co-AAc) microgels as microreactors. A diagrammatic representation of all events occurring during the in situ synthesis of nanoparticles within microgels is shown in Figure 3. The p(NIPAM-co-AAc) microgels are crosslinked and porous. The dimensions of sieves of microgels fall into the nano range. Therefore, microgels are considered to be ideal for the synthesis of particles having nano dimensions.⁴⁴ The p(NIPAM-co-AAc) microgels are co-polymers of NIPAM and AAc. AAc is an acidic monomer that ionizes when the pH of the medium is greater than its pK_a value (~ 4.25).⁴⁵ First of all, the pH of the solution was increased above 4.25 using a base like sodium hydroxide, so that carboxyl groups ($-\text{COOH}$) are ionized and converted into negatively charged carboxylate ions ($-\text{COO}^-$). Then AgNO_3 is added to the reaction mixture. AgNO_3 ionizes and gives positively charged silver ions (Ag^+). Silver ions are counter ions of carboxylate ions; so silver ions are attracted toward carboxylate ions due to electrostatic attraction. This electrostatic attraction makes the silver ions diffuse from outside to inside of micro gel. As AAc units are homogeneously distributed within the network of p(NIPAM-co-AAc) microgels, all silver ions do not accumulate within one sieve. Therefore, it is clear that silver ions are diffused into the whole network of microgels. After addition of AgNO_3 , NaBH_4 is added to the reaction mixture, which reduces silver ions to silver atoms. All silver atoms present in a sieve of microgels coalesce and form a Ag nanoparticle. In this way, growth of Ag nanoparticles occurs in every sieve of microgel particles. As AAc are homogeneously distributed within the whole network of microgel particles and all sieves are of almost the same size, the nanoparticles formed in every sieve are almost the same size. Microgels also prevent growth of nanoparticles

into bigger particles. The polymer network hinders movement of nanoparticles from one sieve to another. In addition, carboxylate ions act as chelating agent for holding Ag nanoparticles within a sieve. Both these factors prevent aggregation of nanoparticles into bigger particles. Zhang et al., Lu et al., and Mohan et al. proposed the same mechanism for in situ synthesis of nanoparticles within microgels by chemical reduction.^{28,44,46}

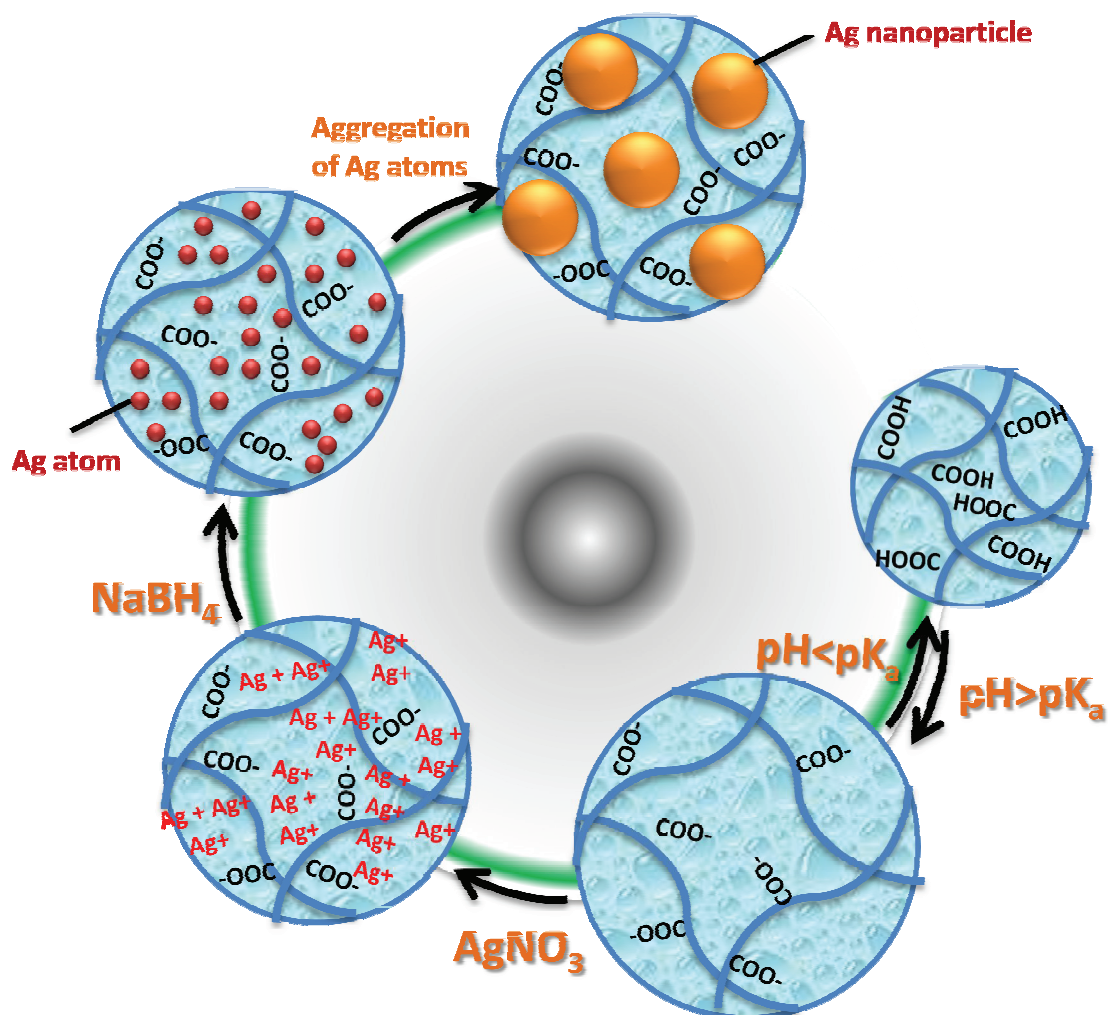


Figure 3. Diagrammatic representation of in situ synthesis of nanoparticles within microgels by chemical reduction of Ag ions.

2.4. Effect of mol percentage of AAc on the size of in vivo synthesized silver nanoparticles

UV-Visible spectra of 1-AAc-Ag, 3-AAc-Ag, 5-AAc-Ag, and 7-AAc-Ag hybrid microgels at pH 10.37 and temperature 18 °C are shown in Figure 4. The values of λ_{SPR} and absorbance at λ_{SPR} are listed in Table 1. It is revealed from Figure 4 and Table 1 that the value of λ_{SPR} and absorbance at λ_{SPR} increase with an increase in the mol percentage of AAc in microgels.

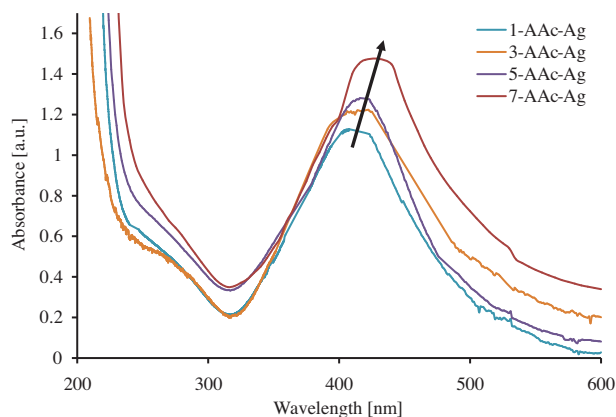


Figure 4. UV-Visible spectra of dilute dispersion of Ag-p(NIPAM-co-AAc) hybrid microgels at pH 10.37 and temperature 18 °C.

Table 1. Values of λ_{SPR} and absorbance at λ_{SPR} for all hybrid microgels samples at pH 10.37 and temperature 18 °C.

Hybrid microgel samples	λ_{SPR} (nm)	Absorbance (a.u.)
1-AAc-Ag	403.2	1.114
3-AAc-Ag	409.1	1.216
5-AAc-Ag	414.0	1.276
7-AAc-Ag	430.0	1.475

The single peak in all spectra confirms that silver nanoparticles synthesized within all microgel samples are spherical.⁴⁶ Spectra of all samples of hybrid microgels are different in position, height, and broadness of peak in Figure 4, which indicates that size, size distribution, and number of Ag nanoparticles is not the same within all hybrid microgel samples. The value of λ_{SPR} increases from 403.2 to 430 nm with an increase in the mol percentage of AAc from 1% to 7%. This means that the size of Ag nanoparticles increases with an increase in the feed content of AAc. When the content of AAc in feed composition increases, the number of carboxyl groups incorporated within microgels also increases. As the pH of the reaction mixture during nanoparticle fabrication was maintained at 8.98 ($8.98 > pK_a$ of AAc (4.25)),⁴⁷ carboxyl groups were in ionized form. Due to electrostatic repulsion among negatively charged carboxylate ions ($-\text{COO}^-$), microgels swell up.⁹ The force of electrostatic repulsion is greater in 7-AAc microgels as compared to 1-AAc microgels, because the 7-AAc sample has high feed contents of AAc. Thus the hydrodynamic radius of microgel samples having high feed of AAc is greater in swollen state as compared to those samples having low feed of AAc.⁴⁸ Thus the number of silver ions entered inside the network increases because an increase in AAc feed contents increases the swelling ratio of micro gels and electrostatic attraction between positively charged silver ions and negatively charged carboxylate ions. Thus the number of silver ions diffused into the 7-AAc sample is greater than those into 1-AAc. In this way, nanoparticles of greater size are synthesized within microgels containing high mol percentage of AAc as compared to those microgels having low mol percentage of AAc. Zhang et al. reported that a red shift in λ_{SPR} takes place when the size of nanoparticles is increased.⁴⁹ They observed a red shift in λ_{SPR} when the size of Au nanoparticles was increased from 24.1 ± 1.7 to 44 ± 5 nm. Similarly, Wu et al. observed that the value of λ_{SPR} increases from 529 to 573 nm by increasing the size of Au nanoparticles from 15 to 95 nm.⁵⁰ It is well known that peak broadness depends upon the size distribution of nanoparticles. Thus content

of AAc not only affects the size of nanoparticles here, but size distribution of Ag nanoparticles is also affected. It is shown in Figure 4 that the peak of λ_{SPR} changes from a sharp to a broader peak when mol percentage of AAc increases from 1% to 7%. Thus the majority of nanoparticles within the 1-AAc-Ag sample are of similar sizes, but nanoparticles fabricated in 7-AAc-Ag have broad size distribution. In the case of the 7-AAc-Ag hybrid system nanoparticles can easily diffuse and get aggregated, and thus it gives a broad distribution of nanoparticles. Therefore, the peak of λ_{SPR} gets broader due to aggregation on increasing content of AAc. The full width at half maximum of spectra of 1-AAc-Ag is 133.1 nm but that for spectra of 7-AAc-Ag is 175 nm, which indicates the size distribution broadening with an increase in feed contents of AAc. Absorbance at λ_{SPR} also increases with an increase in AAc content (Figure 4). This increase in absorbance occurs due to an increase in the size of Ag nanoparticles with an increase in feed contents of AAc.^{51–53} Jana et al. synthesized gold nanoparticles of different sizes ranging from 5.5 to 37 nm by variation of seed to metal salt and calculated the values of their molar extinction coefficients.⁴⁸ They found that the value of the molar extinction coefficient increases with an increase in the size of nanoparticles. Our results are in good agreement with these results. Therefore, the increase in absorbance with an increase in acrylic acid feed contents is due to an increase in the size of Ag nanoparticles.

2.5. Catalytic reduction of p-nitrophenol

Reduction of p-NP to p-AP was used as a model reaction to investigate the catalytic activity of all samples of hybrid microgels here. Figure 5 shows the spectra of the catalytic reduction of p-NP by 1-AAc-Ag microgels scanned at different time intervals. All spectra scanned during the whole time of the reaction have only 2 peaks. This means that no other product is formed during the reaction. Absorbance at 400 nm decreases with time, while absorbance at 300 nm increases with time. This concomitant change in absorbance at 400 and 300 nm shows that catalytic reduction is taking place. It also indicates that concentration of p-NP decreases in the reaction mixture with the passage of time, while concentration of p-AP increases with the passage of time.

Plots of $\ln(A_t/A_o)$ as a function of time for reduction of p-NP catalyzed by hybrid microgel samples are shown in Figure 6. Initially the value of $\ln(A_t/A_o)$ remains constant with the passage of time in these plots, and then it decreases with time. The time during which the value of $\ln(A_t/A_o)$ does not change with the passage of time is called the induction period of the reaction. It means that the reaction is not occurring in this period. Diffusion of p-NP and reducing agent and removal of the silver oxide layer around nanoparticles occur during this time. The induction period is different for all samples (Table 2). Values of induction time duration for all samples are given in Table 2. The values in Table 2 and Figure 7 show that the duration of induction time decreases with an increase in the feed content of AAc. It is well known that the swelling ratio of p(NIPAM-co-AAc) microgels increases with an increase in AAc content.³⁴ Therefore, the size of microgel particles of sample 7-AAc-Ag is greater than that of 1-AAc-Ag microgel sample at pH 10.37. The polymer network around metal nanoparticles is not more compact in the case of 7-AAc-Ag as compared to 1-AAc-Ag. The reactants can diffuse easily through the network towards the catalyst surface in the 7-AAc-Ag sample. However, in case of 1-AAc-Ag, the reactants face some hindrance to approach the catalyst. That is why the value of induction time decreases with an increase in AAc feed contents (Figure 7).

Figure 8 also shows that values of $\ln(A_t/A_o)$ linearly decrease with the passage of time after induction time. This indicates that reduction has started and follows pseudo-first order kinetics. The slope of the linear regions of the plot of $\ln(A_t/A_o)$ versus time gives the value of the apparent rate constant (k_{app}) of reduction. This region of the plot of $\ln(A_t/A_o)$ as a function of time is shown separately in Figure 8. The slope of the plot

was used for determination of k_{app} using a pseudo-first order kinetic model. Figure 8 shows that the slope is different for all samples. Therefore, values of k_{app} for 1-AAc-Ag, 3-AAc-Ag, 5-AAc-Ag, and 7-AAc-Ag hybrid microgel catalyzed reduction are different (Table 2).

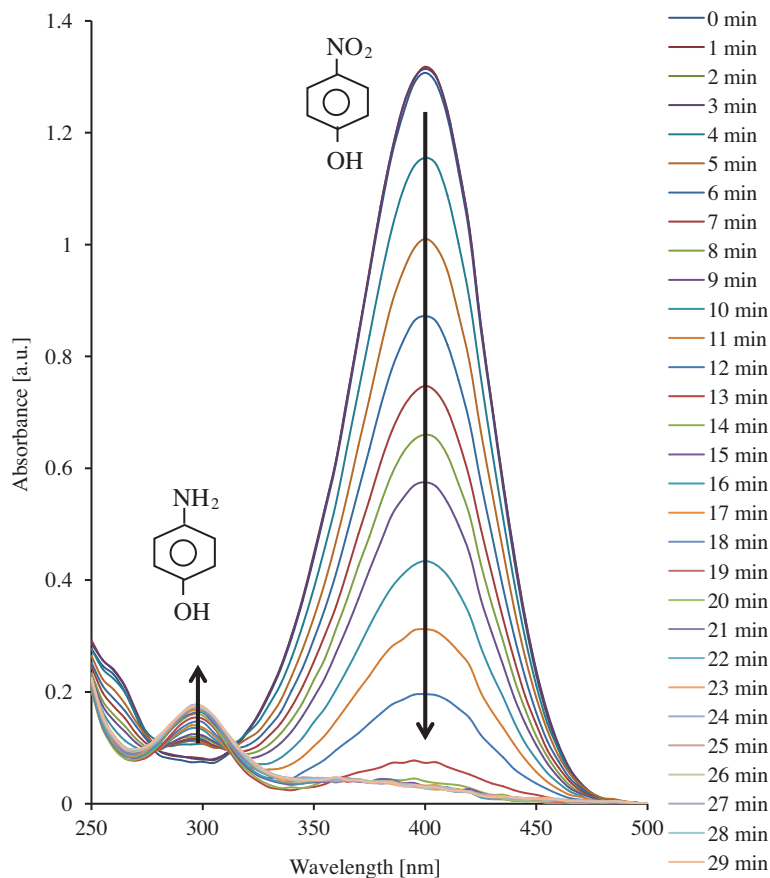


Figure 5. UV-Visible spectra of catalytic reduction of p-NP at temperature 21 °C and pH 9.90. Conditions: $[\text{NaBH}_4] = 124 \text{ mM}$, $[\text{p-NP}] = 0.064 \text{ mM}$ in the presence of 0.1 mL of 55% diluted 1-AAc-Ag hybrid microgels with total volume 2.5 mL.

Table 2. Values of rate constant and induction time for reduction of p-NP catalyzed by different samples of hybrid microgel.

Samples of hybrid microgel	Induction time (min)	k_{app} (min^{-1})
1-AAc-Ag	8.8	0.226
3-AAc-Ag	6.7	0.185
5-AAc-Ag	6.3	0.142
7-AAc-Ag	2.6	0.109

2.6. Effect of feed content of acrylic acid on value of apparent rate constant

Figure 9 shows the plot of k_{app} as a function of mol percentage of AAc. This plot indicates that the value of k_{app} decreases from 0.226 to 0.109 min^{-1} when mol percentage of AAc increases from 1% to 7%. This decrease in the value of k_{app} is linked to the size of nanoparticles fabricated within microgels. Nanoparticles

of greater size are present in microgels having a high content of AAc. Catalysis is a surface phenomenon and larger nanoparticles have a smaller surface area as compared to smaller nanoparticles. Therefore, the rate of catalysis decreases with an increase in feed contents of AAc. In addition, aggregation of nanoparticles within a sample having a high content of AAc may cause a reduction in surface available for catalysis. Thus a decrease in the value of k_{app} is observed with an increase in AAc content. Interestingly, the value of k_{app} decreases linearly with an increase in feed contents of AAc, which can be helpful for quantitative analysis of microgels to determine the AAc feed contents in the sample.

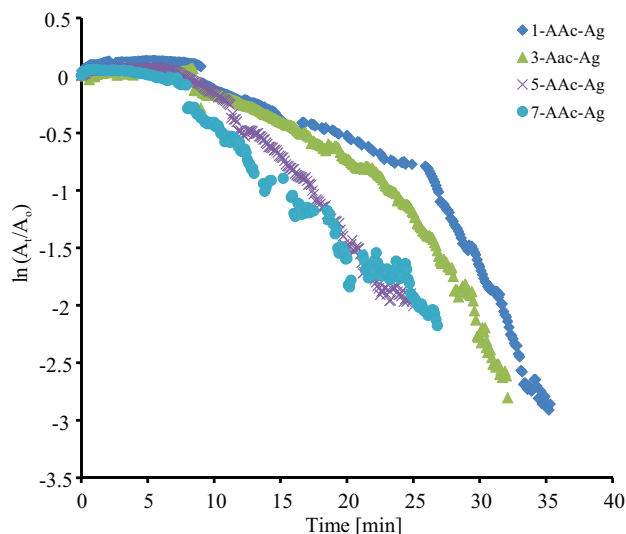


Figure 6. Plot of $\ln(A_t/A_o)$ versus time for reduction of p-NP catalyzed by different samples of hybrid microgels.

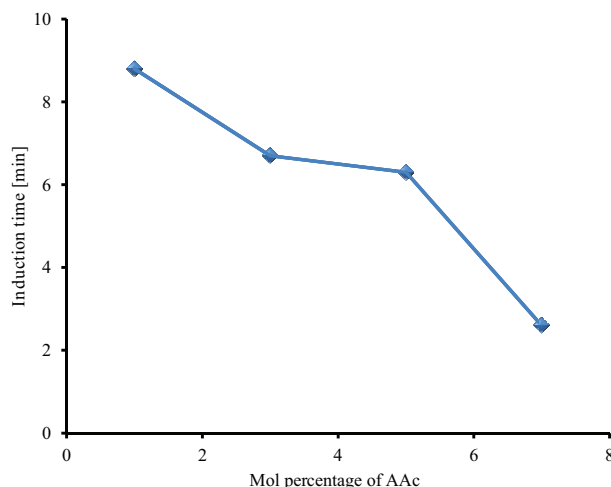


Figure 7. Plot of mol percentage of AAc versus induction time observed during catalytic reduction of p-NP.

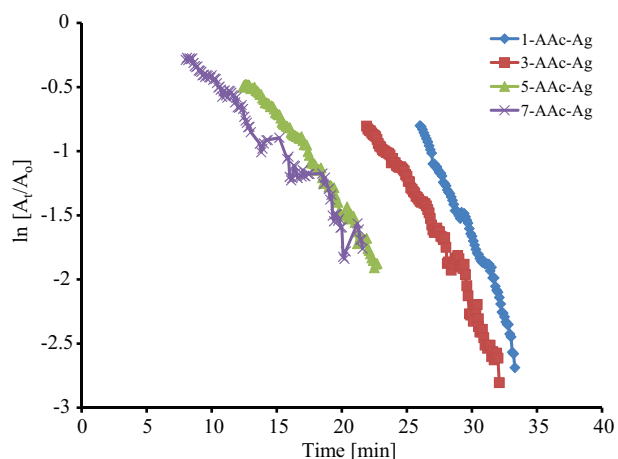


Figure 8. The plot of $\ln(A_t/A_o)$ as a function of time (after induction time) for determination of apparent rate constant of p-NP.

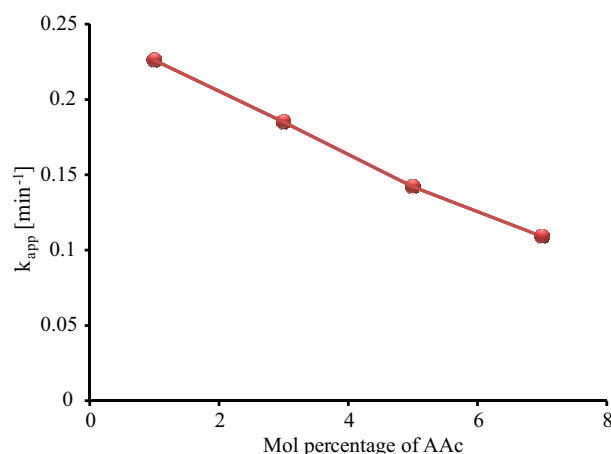


Figure 9. Dependence of k_{app} of catalytic reduction of p-NP on mol percentage of AAc.

3. Experimental

3.1. Materials

Sodium borohydride (NaBH_4) was obtained from Scharlau Company, while acrylic acid (AAc), N-isopropylacrylamide (NIPAM), *N,N*-methylenebis(acrylamide) (BIS), sodium dodecylsulfate (SDS), and p-nitrophenol (p-NP) were purchased from Sigma-Aldrich. Only AAc was purified, by passing through alumina to remove inhibitor under reduced pressure.

3.2. Synthesis of p(NIPAM-co-AAc) microgels

All samples of microgels were prepared by surfactant free precipitation polymerization as reported previously by our group.^{43,51,54,55} Monomers, NIPAM and AAc, crosslinker BIS, and surfactant SDS were dissolved in 95 mL of distilled water in a 3-necked round bottom flask. Then this solution was purged with nitrogen gas at 70 °C for 30 min with constant stirring. Then 5 mL of 0.05 M ammonium persulfate was added dropwise to this mixture. After this, the reaction mixture was continuously stirred at 70 °C for 4 h. Later synthesized p(NIPAM-co-AAc) microgels were cooled and dialyzed using Spectra/Por molecular porous membrane tubing (Fisher Scientific) having MWCO 12,000–140,00 for 1 week against daily exchange of water. Total number of mol was 0.01. The feed compositions of all prepared p(NIPAM-co-AAc) microgels are listed in Table 3.

Table 3. Feed compositions of p(NIPAM-co-AAc) microgels.

Microgel samples	Mol % of NIPAM	Mol % of BIS	Mol % of AAc	SDS (g)
1-AAc	94	5	1	0.05
3-AAc	92	5	3	0.05
5-AAc	90	5	5	0.05
7-AAc	88	5	7	0.05

3.3. Synthesis of Ag-p(NIPAM-co-AAc) hybrid microgels

First, 14, 36, and 0.4 mL of pure microgel dispersion, water, and AgNO_3 solution (0.1 M), respectively, were added to a 3-necked round bottom flask. After continuous stirring for 30 min under atmosphere of nitrogen gas, 5 mL of NaBH_4 solution (0.01 g/5 mL) was added to this mixture. Then this reaction mixture was stirred for 90 min. Later the hybrid microgels were dialyzed for 1 h against twice exchange of water. 1-AAc-Ag, 3-AAc-Ag, 5-AAc-Ag, and 7-AAc-Ag hybrid microgel samples were prepared from 1-AAc, 3-AAc, 5-AAc, and 7-AAc microgels, respectively, by using the above method. Moreover, pH of the reaction mixture was maintained at 8.98 before addition of reducing agent for preparation of all samples of hybrid microgels.

3.4. Catalytic reduction of p-nitrophenol

First, 2 mL of p-NP (0.08 mM), 0.4 mL of NaBH_4 (77.5 mM), and 0.1 mL of hybrid microgels (55% diluted) were taken in a cuvette for study of reduction of p-NP. The reaction was monitored by UV-Visible spectrophotometry using a UVD 3500 (Labomed Inc.). The spectra were scanned in the range of wavelength of 200–500 nm at a fixed time interval up to the completion of the reaction at 21 °C.

3.5. Characterization

An RX I FTIR spectrometer (PerkinElmer) was used to obtain FTIR spectra in the near infrared range of 4000–650 cm^{-1} . A 90Plus particle size analyzer (Brookhaven, USA) equipped with a solid-state laser (wavelength = 659 nm) and a power of 15 mW was used to measure the size of particles at an angle of 90° in aqueous solution. A UVD 3500 (Labomed Inc.), was used for UV-Visible studies.

4. Conclusions

In this study, we investigated the impact of the feed contents of acrylic acid on the size and size distribution of silver nanoparticles fabricated inside microgels. These hybrid microgels were used as catalysts to investigate the effect of the feed contents of acrylic acid on the value of induction time and apparent rate constant of p-nitrophenol. The red shift in surface plasmon resonance wavelength confirms that the size of in vivo synthesized silver nanoparticles increases with an increase in the contents of acrylic acid. The increase in full width at half maxima with an increase in acrylic acid contents indicates broadening of size distribution with an increase in acrylic acid contents. The value of the apparent rate constant of the catalytic reduction of p-nitrophenol decreases with an increase in the mol percentage of acrylic acid. This decrease is due to the increase in the size of nanoparticles with an increase in the content of acrylic acid. The linear decrease in the value of the apparent rate constant with feed contents of acrylic acid has a potential to be used for quantitative determination of the feed contents of acrylic acid in microgels.

Acknowledgment

This work was supported by University of the Punjab Lahore, Pakistan, under university grant for Fiscal Year 2013–2014.

References

1. Liu, W.; Yang, X.; Huang, W. *J. Colloid Interface Sci.* **2006**, *304*, 160–165.
2. Dokoutchaev, A.; James, J. T.; Koene, S. C.; Pathak, S.; Prakash, G. S.; Thompson, M. E. *Chem. Mater.* **1999**, *11*, 2389–2399.
3. Gaikwad, A. V.; Holuigue, A.; Thathagar, M. B.; ten Elshof, J. E.; Rothenberg, G. *Chem. Eur. J.* **2007**, *13*, 6908–6913.
4. Thathagar, M. B.; Beckers, J.; Rothenberg, G. *Adv. Synth. Catal.* **2003**, *345*, 979–985.
5. Thathagar, M. B.; Ten-Elshof, J. E.; Rothenberg, G. *Angew. Chem. Int. Ed.* **2006**, *45*, 2886–2890.
6. Herves, P.; Perez-Lorenzo, M.; Liz-Marzan, L. M.; Dzubielia, J.; Lu, Y.; Ballauff, M. *Chem. Soc. Rev.* **2012**, *41*, 5577–5587.
7. Haruta, M. *Catal. Today* **1997**, *36*, 153–166.
8. Ajmal, M.; Farooqi, Z. H.; Siddiq, M. *Korean J. Chem. Eng.* **2013**, *30*, 2030–2036.
9. Khan, S. R.; Farooqi, Z. H.; Ajmal, M.; Siddiq, M.; Khan, A. *J. Disp. Sci. Technol.* **2013**, *34*, 1324–1333.
10. Antoine, O.; Bultel, Y.; Durand, R. *J. Electroanal. Chem.* **2001**, *499*, 85–94.
11. Gu, Y.; Zhang, Y.; Zhang, F.; Wei, J.; Wang, C.; Du, Y.; Ye, W. *Electrochim. Acta* **2010**, *56*, 953–958.
12. Sahiner, N.; Ozay, O. *React. Funct. Polym.* **2011**, *71*, 607–615.
13. Du, Y.; Chen, H.; Chen, R.; Xu, N. *Appl. Catal., A* **2004**, *277*, 259–264.
14. Sahiner, N.; Ozay, H.; Ozay, O.; Aktas, N. *Appl. Catal., A* **2010**, *385*, 201–207.
15. Sahiner, N.; Butun, S.; Ozay, O.; Dibek, B. *J. Colloid Interface Sci.* **2012**, *373*, 122–128.

16. Das, J.; Aziz, M. A.; Yang, H. *J. Am. Chem. Soc.* **2006**, *128*, 16022–16023.
17. Lee, J.; Park, J. C.; Song, H. *Adv. Mater.* **2008**, *20*, 1523–1528.
18. Mei, Y.; Lu, Y.; Polzer, F.; Ballauff, M.; Drechsler, M. *Chem. Mater.* **2007**, *19*, 1062–1069.
19. Makarova, O. V.; Rajh, T.; Thurnauer, M. C.; Martin, A.; Kemme, P. A.; Cropek, D. *Environ. Sci. Technol.* **2000**, *34*, 4797–4803.
20. Tada, H.; Ishida, T.; Takao, A.; Ito, S.; Mukhopadhyay, S.; Akita, T.; Tanaka, K.; Kobayashi, H. *Chem. Phys. Chem.* **2005**, *6*, 1537–1543.
21. Wang, H.; Yan, J.; Chang, W.; Zhang, Z. *Catal. Commun.* **2009**, *10*, 989–994.
22. Rashid, M.; Mandal, T. K. *Adv. Funct. Mater.* **2008**, *18*, 2261–2271.
23. Bhattacharya, S.; Eckert, F.; Boyko, V.; Pich, A. *Small* **2007**, *3*, 650–657.
24. Pich, A.; Karak, A.; Lu, Y.; Ghosh, A. K.; Adler, H. P. *J. Nanosci. Nanotechnol.* **2006**, *6*, 3763–3769.
25. Lu, Y.; Proch, S.; Schrunner, M.; Drechsler, M.; Kempe, R.; Ballauff, M. *J. Mater. Chem.* **2009**, *19*, 3955–3961.
26. Astruc, D.; Chardac, F. *Chem. Rev.* **2001**, *101*, 2991–3024.
27. Crooks, R. M.; Zhao, M.; Sun, L.; Chechik, V.; Yeung, L. K. *Acc. Chem. Res.* **2001**, *34*, 181–190.
28. Zhang, J.; Xu, S.; Kumacheva, E. *J. Am. Chem. Soc.* **2004**, *126*, 7908–7914.
29. Liu, Y.; Liu, X.; Yang, J.; Lin, D.; Chen, X.; Zha, L. *Colloids Surf., A* **2012**, *393*, 105–110.
30. Xie, L.; Chen, M.; Wu, L. *J. Polym. Sci., Part A: Polym. Chem.* **2009**, *47*, 4919–4926.
31. Sahiner, N.; Ozay, H.; Ozay, O.; Aktas, N. *Appl. Catal., B* **2010**, *101*, 137–143.
32. Wang, Y.; Wei, G.; Wen, F.; Zhang, X.; Zhang, W.; Shi, L. *J. Mol. Catal. A* **2008**, *280*, 1–6.
33. Jiang, Z.; Liu, C.; Sun, L. *J. Phys. Chem. B* **2005**, *109*, 1730–1735.
34. Kratz, K.; Hellweg, T.; Eimer, W. *Colloids Surf., A* **2000**, *170*, 137–149.
35. Mahmoud, M. A.; Narayanan, R.; El-Sayed, M. A. *Acc. Chem. Res.* **2013**, *46*, 1795–1805.
36. Liu, B.; Wang, Q.; Yu, S.; Zhao, T.; Han, J.; Jing, P.; Hu, W.; Liu, L.; Zhang, J.; Sun, L.; et al. *Nanoscale* **2013**, *5*, 9747–9757.
37. Atae-Esfahani, H.; Nemoto, Y.; Wang, L.; Yamauchi, Y. *Chem. Commun.* **2011**, *47*, 3885–3887.
38. Okada, K.; Maeda, Y. *J. Appl. Polym. Sci.* **2013**, *130*, 201–205.
39. Wang, S. Q.; Liu, Q. L.; Zhu, A. M. *Eur. Polym. J.* **2011**, *47*, 1168–1175.
40. Van Gough, D.; Bunker, B. C.; Roberts, M. E.; Huber, D. L.; Zarick, H. F.; Austin, M. J.; Wheeler, J. S.; Moore, D.; Spoerke, E. D. *ACS Appl. Mater. Interf.* **2012**, *4*, 6247–6251.
41. Yu, S.; Lu, Z.; Chen, Z.; Liu, X.; Liu, M.; Gao, C. *J. Membr. Sci.* **2011**, *371*, 293–306.
42. Yoo, M.; Sung, Y.; Lee, Y.; Cho, C. *Polymer* **2000**, *41*, 5713–5719.
43. Farooqi, Z. H.; Khan, H. U.; Shah, S. M.; Siddiq, M. *Arabian J. Chem.* **2013**, *36*, 423–429.
44. Lu, Y.; Mei, Y.; Schrunner, M.; Ballauff, M.; Möller, M. W.; Breu, J. *J. Phys. Chem. C* **2007**, *111*, 7676–7681.
45. Farooqi, Z. H.; Khan, S. R.; Hussain, T.; Begum, R.; Ejaz, K.; Majeed, S.; Ajmal, M.; Kanwal, F.; Siddiq, M. *Korean J. Chem. Eng.* **2014**, *31*, 1674–1680.
46. Murali Mohan, Y.; Lee, K.; Premkumar, T.; Geckeler, K. E. *Polymer* **2007**, *48*, 158–164.
47. Naeem, H.; Farooqi, Z. H.; Shah, L. A.; Siddiq, M. *J. Polym. Res.* **2012**, *19*, 1–10.
48. Qiu, X.; Kwan, C. M. S.; Wu, C. *Macromolecules* **1997**, *30*, 6090–6094.
49. Zhang, J. Z.; Noguez, C. *Plasmonics* **2008**, *3*, 127–150.
50. Wu, S.; Kaiser, J.; Drechsler, M.; Ballauff, M.; Lu, Y. *Colloid. Polym. Sci.* **2013**, *291*, 231–237.
51. Vongsavat, V.; Vittur, B. M.; Bryan, W. W.; Kim, J.; Lee, T. R. *ACS Appl. Mater. Interf.* **2011**, *3*, 3616–3624.
52. Wu, W.; Zhou, T.; Zhou, S. *Chem. Mater.* **2009**, *21*, 2851–2861.
53. Jana, N. R.; Gearheart, L.; Murphy, C. J. *Langmuir* **2001**, *17*, 6782–6786.
54. Farooqi, Z. H.; Khan, A.; Siddiq, M. *Polym. Int.* **2011**, *60*, 1481–1486.
55. Farooqi, Z. H.; Siddiq, M., *J. Disp. Sci. Technol.* **2014**, *36*, 423–429.